12th International Congress on Artificial Materials for Novel Wave Phenomena – Metamaterials 2018
Espoo, Finland, Aug. 27th – Sept. 1st, 2018

Diffuse THz Scattering via Coding Metasurfaces

C. Koral[1], G. Papari[1,2], A. Andreone[1,2], M. Moccia[3], G. Castaldi[3], V. Galdi[3], S. Liu[4], R.Y. Wu[4], T.J. Cui[4]

[1]Department of Physics, University of Napoli "Federico II", I-80125, Napoli, Italy
[2]CNR-SPIN, UoS Napoli, I-80126, Napoli, Italy
[3]Department of Engineering, University of Sannio, I-82100, Benevento, Italy
[4]State Key Lab. of Millimeter Waves, Southeast University, Nanjing 210096, China
e-mail: can.koral@fisica.unina.it

Abstract **– The Terahertz region covers the electromagnetic spectrum incorporating the advantages of both microwaves and infrared light waves. Many different techniques have been proposed to manipulate THz waves. Among them, metamaterials and metasurfaces have proven to have a high potential to engineer new type of functional THz devices. A recent and promising approach is based on coding metasurfaces, consisting of two or more basic ("digital") unit cells with out-of-phase response, which can be used to achieve diffuse scattering. Here, with special focus on the scattering-signature reduction, the physical mechanism is elucidated via a theoretical study and the relevant scaling-laws validated using THz Time Domain Spectroscopy.**

I. INTRODUCTION

Digital metasurfaces, based on the combination of two basic unit cells with out-of-phase response, have been the subject of many recent studies aimed at achieving diffuse scattering, with potential applications to diverse fields, including radar-signature control and computational imaging [1]. Diffuse-scattering metasurfaces appear to be an attractive solution in view of their potential conformability (by relying on flexible substrates) as well as the negligible impact on the thermal signature (as opposed, e.g., to absorbers). Via a theoretical study of the relevant scaling-laws, we elucidate the physical mechanism underlying the scattering-signature reduction, and we analytically derive some absolute and realistic bounds. Moreover, we introduce a simple, deterministic sub-optimal design strategy that yields results comparable with those typically obtained by approaches based on the brute-force numerical optimization, at a negligible fraction of their computational burden, thereby paving the way to the design of structures with arbitrarily large electrical size. Our results are validated by both rigorous full-wave numerical simulations and experiments at around 1 THz, and may be of interest in a variety of application fields, such as the design of low-scattering targets and illumination apertures for computational imaging, not necessarily restricted to electromagnetic scenarios.

II. THEORETICAL BACKGROUND

The geometrical distribution of the binary elements is based on the Golay-Rudin-Shapiro (GRS) polynomials [2]. The P_ν and Q_ν GRS polynomials can be recursively defined via two intertwined formulas

$$P_{\nu+1}(\xi)=P_\nu(\xi)+\xi^{2^\nu}Q_\nu(\xi),\quad Q_{\nu+1}(\xi)=P_\nu(\xi)-\xi^{2^\nu}Q_\nu(\xi),\qquad \text{with}\quad P_0=Q_0=1. \qquad (1)$$

with ξ denoting a complex-valued (generally unimodular) variable. As theoretically demonstrated [3], GRS polynomials show a flatten response and an impinging wave can be "identically" spread in all directions reducing the backscattered field: by increasing the polynomial order, the metasurface area and the reduction is larger and larger. In Fig. 1a) and b) the response in the *k*-space of GRS polynomials of order 2 and 5 is shown respectively. In Fig. 1c) the resulting scattering profile for two metasurfaces coded using the polynomial P_2 and P_5 is reported.

978-1-5386-4702-8/18/$31.00 ©2018 IEEE

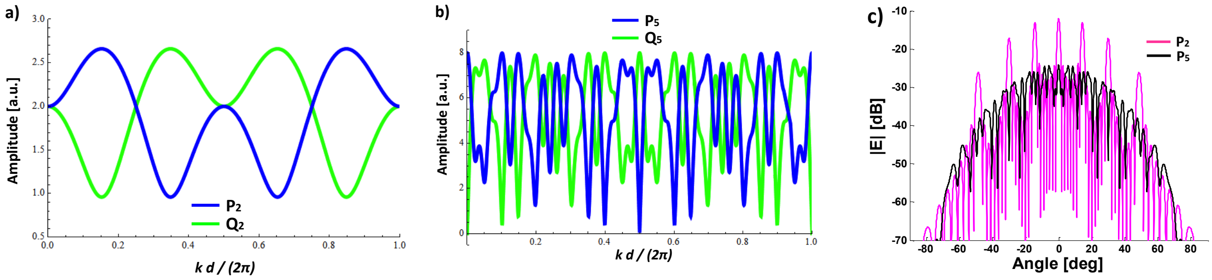

Fig. 1. a) GRS polynomials of order 2; b) GRS polynomials of order 5; c) Scattered E-field for P_2 and P_5.

IV. EXPERIMENTAL STUDY

To experimentally validate the performance of the proposed coding, different samples have been fabricated using a UV photolithographic method. Briefly, the process consists of the e-beam deposition of two 200-nm thick gold films interposed by 20 um polymide layer produced by spin coating [4]. The final pattern on the top surface is formed via a standard lift-off procedure. Each metasurface covers an area of 10 x 10 mm^2, large enough to be fully illuminated by a plane-wave-like incident beam. In Fig. 2(a), the single bit cell based on a golden square patch is shown. The *w* dimension is different for the “0” and “1” bit (30 and 45 um, respectively) and each cell has a periodicity *a* = 50 um. In Fig. 2(b) a picture of a 2” Au layer on silicon wafer is shown, over which 4 different coding metasurfaces have been realised.

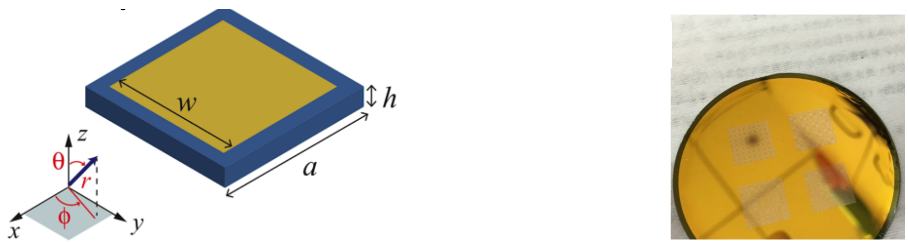

(a) **(b)**

Fig. 2. (a) Square patch with different *w* for “0” and “1” element; (b) Au metasurfaces fabricated on a 2” Si wafer

For the experimental investigation of the response and the physical mechanism underlying the scattering-signature reduction and the characterization of the diffuse scattering from the metasurfaces, we used a customized fiber-coupled THz spectrometer. The system is composed of photoconductive antennas both for THz emission and detection driven by a femtosecond fiber laser @1560nm and pulse length < 90 fs. We have employed various setups to measure the radiation scattered by each metasurface for a normal incident wave.

(a) **(b)** **(c)**

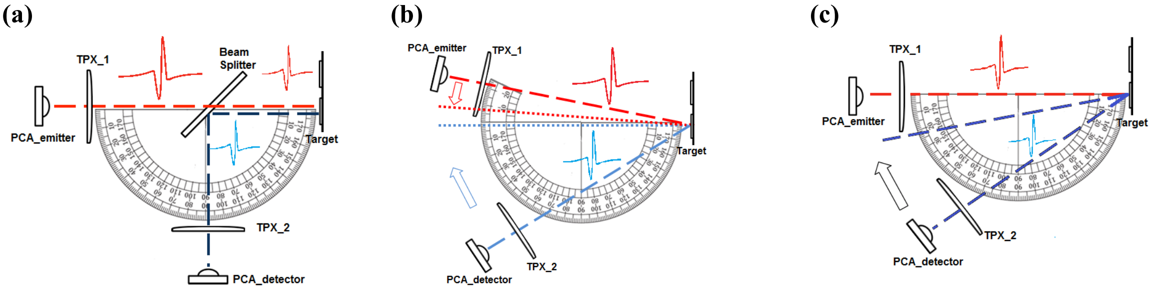

Fig. 3. Scheme for (a) specular, (b) narrow angle (<20°) and (c) large angle (>20°) scattering measurements.

Detection and collection schemes for the specular and angular reflections of the electric field temporal signal are schematically shown in Fig. 3.

By Fourier transforming the time domain signal, we can extract the radar-cross-section (RCS) ratio as a function of frequency and angle for different coding patterns. Representative cuts are shown in Fig. 4(a) and (b) respectively for the GRS P_2-type design.

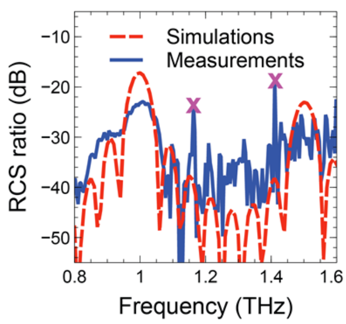

(a)

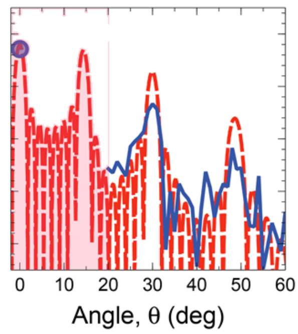

(b)

Fig. 4. Simulated (red-dashed) and measured (blue-solid) RCS ratios as a function of frequency at $\theta = 30°$ (a) and reflection angle at $f = 1$ THz (b) for the P_2-coded metasurface. The magenta-cross markers in panel (a) indicate the water-vapor absorption peaks. The pink-shaded area in panel (b) indicates a 20° angular "blind" region not accessible by the detector.

III. Conclusions

In this work the functionalities of a coding metasurface for diffuse scattering has been theoretically and experimentally demonstrated in the THz spectrum. Based on the GRS polynomial coding, a digital metasurface has been designed and tested confirming the predicted backscattering reduction. The attainable RCS as a function of angle and frequency for different coding patterns is extracted from the THz-TDS measurements by applying different detection and collection schemes for the specular and angular reflections. Experimental results show that it is possible to achieve diffuse scattering on relatively small metasurfaces by using GRS-coding. This mechanism may pave the way to an alternative approach for the control of electromagnetic scattering and for the development of new type of functional THz devices.

References

[1] T. J. Cui *et al.,* "Coding metamaterials, digital metamaterials and programmable metamaterials ," *Light Sci. Appl.,* vol. 3, p. e218, 2014.
[2] W. Rudin, "Some theorems on Fourier coefficients," *Proc. Am. Math. Soc.*, vol. 10, p. 855, 1959.
[3] M. Moccia *et al.*, "Coding Metasurfaces for Diffuse Scattering: Scaling Laws, Bounds, and Suboptimal Design," *Adv. Opt. Mat.*, vol. 5, p. 1700455, 2017.
[4] S. Liu *et al.*, "Anisotropic coding metamaterials and their powerful manipulation of differently polarized terahertz waves," *Light Sci. Appl.*, vol. 5, p.e16076, 2016.